High-speed tracking control of piezoelectric actuators using an ellipse-based hysteresis model

GuoYing Gu and LiMin Zhu[a)]
State Key Laboratory of Mechanical System and Vibration, School of Mechanical Engineering, Shanghai Jiao Tong University, Shanghai 200240, China

(Received 20 May 2010; accepted 5 July 2010; published online 11 August 2010)

In this paper, an ellipse-based mathematic model is developed to characterize the rate-dependent hysteresis in piezoelectric actuators. Based on the proposed model, an expanded input space is constructed to describe the multivalued hysteresis function $H[u](t)$ by a multiple input single output (MISO) mapping $\Gamma: R^2 \rightarrow R$. Subsequently, the inverse MISO mapping $\Gamma^{-1}(H[u](t), H[\dot{u}](t); u(t))$ is proposed for real-time hysteresis compensation. In controller design, a hybrid control strategy combining a model-based feedforward controller and a proportional integral differential (PID) feedback loop is used for high-accuracy and high-speed tracking control of piezoelectric actuators. The real-time feedforward controller is developed to cancel the rate-dependent hysteresis based on the inverse hysteresis model, while the PID controller is used to compensate for the creep, modeling errors, and parameter uncertainties. Finally, experiments with and without hysteresis compensation are conducted and the experimental results are compared. The experimental results show that the hysteresis compensation in the feedforward path can reduce the hysteresis-caused error by up to 88% and the tracking performance of the hybrid controller is greatly improved in high-speed tracking control applications, e.g., the root-mean-square tracking error is reduced to only 0.34% of the displacement range under the input frequency of 100 Hz. © *2010 American Institute of Physics.* [doi:10.1063/1.3470117]

I. INTRODUCTION

Because of the large output force, high bandwidth, and fast response time, piezoelectric actuators are gaining popularity in many micro- and nanopositioning applications such as atomic force microscopes,[1] scanning tunneling microscopes,[2] and micromanipulation.[3,4] However, the piezoelectric material exhibits inherent nonlinearities such as creep and hysteresis[5] as shown in Fig. 1, which drastically degrade the positioning performance of piezoelectric actuators.

Creep is the drift of the output displacement for a constant applied voltage, which becomes significant over extended periods of time during low-speed operations. This phenomenon can be characterized by a definite mathematic model. Jung and Gweon[6] discussed the creep characteristics of piezoelectric actuators in detail, and Jung *et al.*[7] demonstrated that the creep could be compensated by the closed proportional integral differential (PID) controller. However, in high-speed scanning applications, the creep effect can be neglected.[8]

Hysteresis effect is the multivalued nonlinear phenomenon between the applied voltage and the output displacement. The maximum error caused by the hysteresis can be as much as 15% of the travel range if the piezoelectric actuators operate in the open-loop strategy.[9] Particularly, the hysteresis nonlinearity is rate-dependent, which becomes more evident with the increase of input frequencies and amplitudes as shown in Fig. 2. The phenomenon well corresponds to the recent experimental reports.[10,11] Although the charge control[12] instead of voltage control achieved almost linear response of the piezoelectric actuators, it has not been widely used because of the complicated circuitry of the power driver.[13] Therefore, effective methodologies for modeling and control of the hysteresis, which can improve the tracking performance and bandwidth, have drawn significant research interest recently.

To characterize the hysteresis behavior, many mathematic models have been developed such as the Bouc–Wen model, Duhem model, Maxwell model,[14] backlashlike model,[15] Preisach model,[9] and Prandtl–Ishlinskii model (PIM).[16] Readers may refer to Refs. 17 and 18 for reviews of the hysteresis models. Such models have been widely applied to design controllers for hysteresis compensation of the piezoelectric actuators. Ge and Jouaneh[9] proposed a feedforward controller to cancel the hysteresis based on the classical Preisach model. They also designed a PID feedback controller to improve the tracking precision. The same control technique could also be found in Refs. 19 and 20. As a superposition of elementary play or stop operators, the PIM is widely adopted to compensate for the hysteresis in applications.[3,16,21] However, these models consist of many weighted fundamental operators and are computationally complex for real-time implementation. Efforts have also been made to develop simpler hysteresis models. Third-order polynomials are proposed to describe the hysteresis and inverse polynomial-model-based controllers are designed to linearize the hysteresis.[22–24] A simple phase control approach

[a)]Electronic mail: zhulm@sjtu.edu.cn.

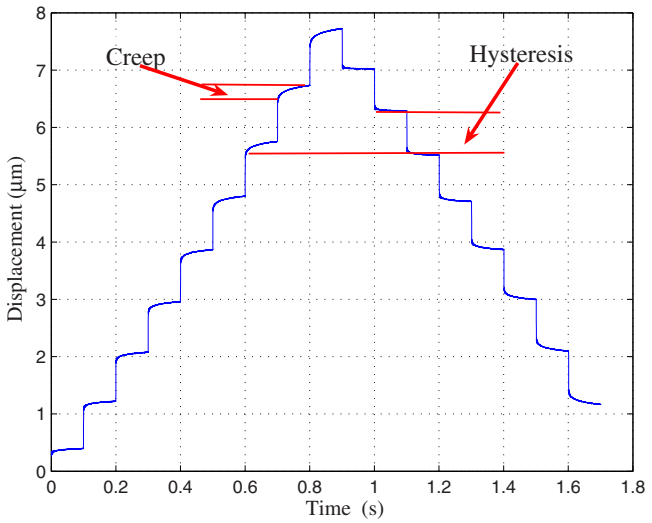

FIG. 1. (Color online) Output displacement of the piezoelectric actuator driven by the input voltage.

is proposed for hysteresis reduction in Ref. 25, which concludes that the phase angle due to the hysteresis only depends on the amplitude of the input signal but not on the frequency.

The aforementioned hysteresis models are originally developed to describe the rate-independent hysteresis and successfully predict the hysteresis behavior at lower input frequencies. However, the hysteresis of the piezoelectric actuators is a rate-dependent phenomenon, strongly depending on frequencies and amplitudes of the control input. Although recent progresses[26–28] have been carried out to modify the Preisach model and PIM to predict the rate-dependent hysteresis with varying rates of input or output, the expressions of the dynamic density functions in these models remain complex and their parameters are difficult to estimate. For high-speed tracking control of the piezoelectric actuator-based nanopositioning systems,[8] many advanced control strategies such as vibration control,[29] damping control,[30] and iterative learning control[4] have also been proposed. However, the rate-dependent hysteresis is not considered in the literature and results are produced only for designing controllers of a dynamical system.

In this work, an ellipse-based mathematic model is proposed to characterize the rate-dependent hysteresis in piezoelectric actuators. In controller design, a model-based feedforward controller in conjunction with a PID feedback loop is developed for high-speed tracking control of the piezoelectric actuators. Experimental results show that the tracking control accuracy with hysteresis compensation is greatly improved in high-speed applications over that without hysteresis compensation. The remainder of this paper is organized as follows. In the next section, the new mathematic model is proposed to describe the rate-dependent hysteresis. In Sec. III, we illustrate the experiment platform, and in Sec. IV, we present the proposed tracking control schemes. Then, in Sec. V, we show and discuss the experimental results, and Sec. VI concludes the paper.

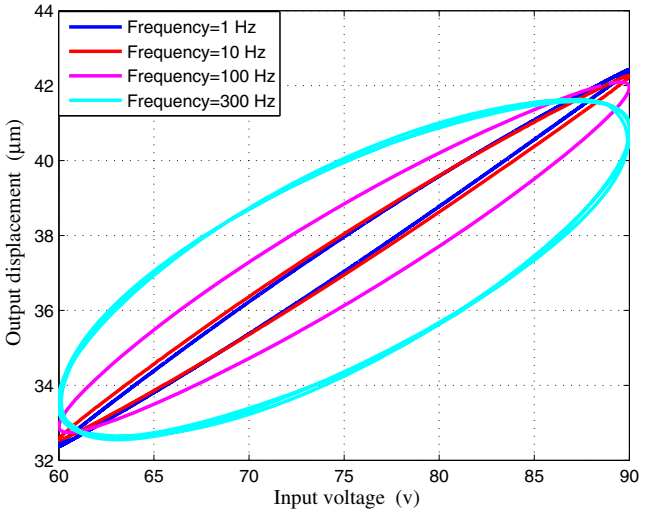

(a) Different frequencies under a fixed amplitude.

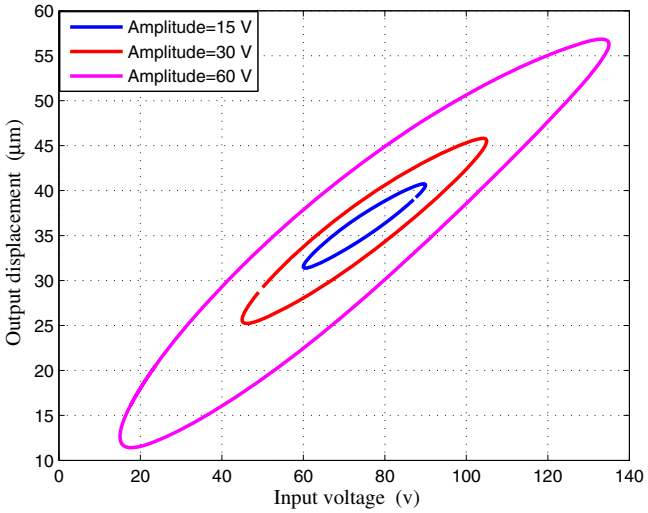

(b) Different amplitudes under a fixed frequency.

FIG. 2. (Color online) Rate-dependent hysteresis curves excited by the sinusoidal input voltage with a positive 75 V bias.

II. AN ELLIPSE-BASED HYSTERESIS MODEL

Elliptical models are important geometric primitives in the fields of pattern recognition and computer vision,[31] and are also used in magnetization modeling.[32] However, little is known about in hysteresis modeling for piezoelectric actuators. In this work, we use elliptical models to describe the rate-dependent hysteresis behaviors in the piezoelectric actuators. The proposed model is efficient because the expressions of the ellipses are completely analytical and can be determined easily by a set of parameters.[33]

Suppose that data points $X_i=(x_i,y_i)^T, i\in[1,2,\ldots]$ are given in an ellipse. These points can be described in the parametric form[31]

$$X_i = X_0 + R(\phi)AP(\theta_i), \tag{1}$$

where $X_0=(x_c,y_c)^T$ are the coordinates of the center, $R(\phi)=\begin{pmatrix}\cos\phi & -\sin\phi\\ \sin\phi & \cos\phi\end{pmatrix}$, $A=\mathrm{diag}(a,b),(a>b)$, and $P(\theta_i)=(\cos\theta_i,\sin\theta_i)^T$. $R(\phi)$ is the rotation matrix, where ϕ is the orientation of the ellipse between the major axis and the x-axis in the two-dimensional plane. a and b are the lengths

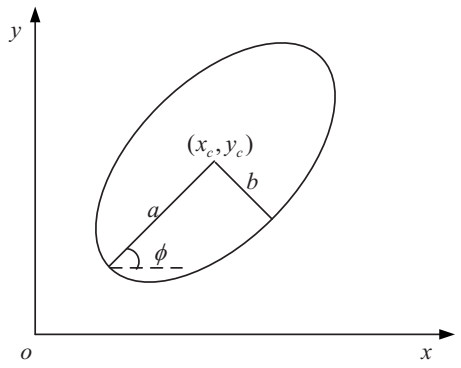

FIG. 3. The illustration of an ellipse.

of the major and minor radii, respectively. $P(\theta_i)$ is the parametric matrix with θ_i varying from 0 to 2π. Obviously, there is a one-to-one mapping between the x_i and y_i by introducing the parameter θ_i. The parameters of the ellipse are also illustrated in Fig. 3.

In this work, we use the x-axis coordinate of the ellipse to represent the control input $u(t)$ described by Eq. (1), while the y-axis coordinate represents the output displacement $y(t)$. Hence, we obtain the following set of equations:

$$\begin{cases} u(t) = u_0 + u_A \sin(2\pi ft + \alpha_1) \\ y(t) = y_0 + y_A \sin(2\pi ft + \alpha_2), \end{cases} \tag{2}$$

where $u_A = \sqrt{a^2 \cos^2 \phi + b^2 \sin^2 \phi}$, $y_A = \sqrt{a^2 \sin^2 \phi + b^2 \cos^2 \phi}$, $2\pi ft = \theta$, $\alpha_1 = \arctan[(b/a)\tan \phi]$, $\alpha_2 = \arctan[(-b/a)\cot \phi]$, and $\alpha_2 < \alpha_1$. Therefore, the multivalued hysteresis is described by a continuous one-to-one mapping $\Gamma(\cdot)$ between the input voltage $u(t)$ and the output displacement $y(t)$ based on the elliptic model. Figure 4 shows the block diagram of the new hysteresis model. As discussed in Ref. 34, the ellipse-based hysteresis model is efficient and accurate to characterize the rate-dependent hysteresis.

Remark 1. *Based on the developed hysteresis model, an expanded input space is constructed to describe the multivalued hysteresis function $H[u](t)$ by a continuous one-to-one mapping $\Gamma: R^2 \rightarrow R$.*

III. EXPERIMENTAL SETUP

As shown in Fig. 5, an experimental platform is built in this work for tracking control of the piezoelectric actuators. A preloaded piezoelectric stack actuator (PPSA) PSt 150/7/100 VS12 from Piezomechanik in Germany is adopted to drive the one-dimensional flexure hinge guiding nanopositioning stage. The resonance frequency of the PPSA is 10 kHz and a high-resolution strain gauge position sensor (SGPS) integrated in the PPSA is used to measure the stage position. The SGPS provides 67.66 μm of travel range with the sensitivity of 0.148 V/μm. The real-time displacement

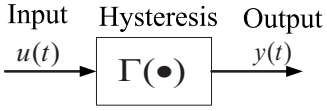

FIG. 4. Block diagram of the new hysteresis model.

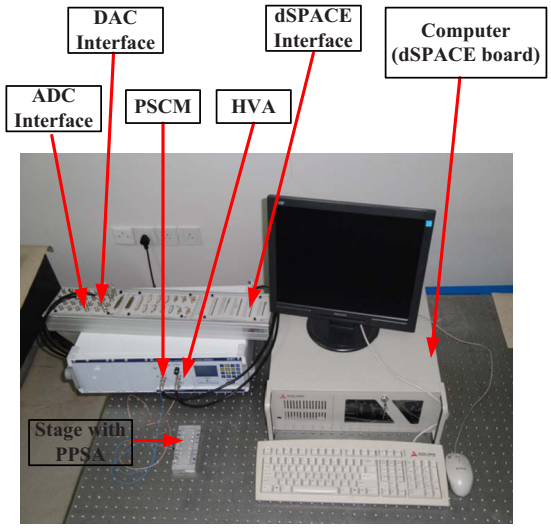

FIG. 5. (Color online) The experimental platform.

is captured by the position servo-control module and then fed into a 16-bit analog-to-digital converter (ADC). At the same time, a 16-bit digital-to-analog converter (DAC) is used to generate various analog excitations to drive the PPSA. The excitation signals are amplified by a high-voltage amplifier with a fixed gain of 15, which provides excitation voltage for the PPSA in the 0–150 V range. In this work, both the ADC and DAC are equipped in the DSPACE-DS1103 rapid prototyping controller board, which is used to implement the proposed control strategy. The sampling frequency of the system is set to 10 kHz. In the controller design using the DSPACE, the excitation voltage for the PPSA is normalized to 0–1 V with respect to the 0–150 V range, while the real-time displacement signal is normalized with the maximum displacement of 67.66 μm.

IV. CONTROLLER DESIGN

We use a hybrid control strategy combining a model-based feedforward controller and a PID feedback loop for high-accuracy and high-speed tracking control of piezoelectric actuators. The feedforward controller is developed to cancel the rate-dependent hysteresis based on the inverse hysteresis model, while the PID controller is used to compensate for the creep, modeling errors, and parameter uncertainties. The DSPACE-DS1103 rapid prototyping control board is used for real-time implementation of the control strategies. SIMULINK and MATLAB are adopted to download the designed controllers into the DSPACE board. Figure 6 shows the block diagram of the hybrid control scheme.

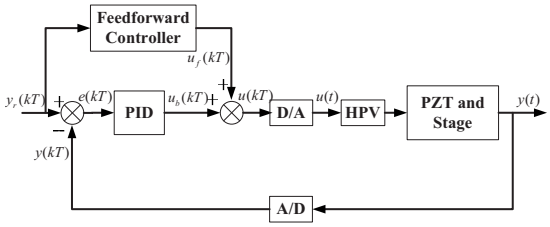

FIG. 6. Block diagram of the hybrid control scheme combining a model-based feedforward controller and a PID feedback loop.

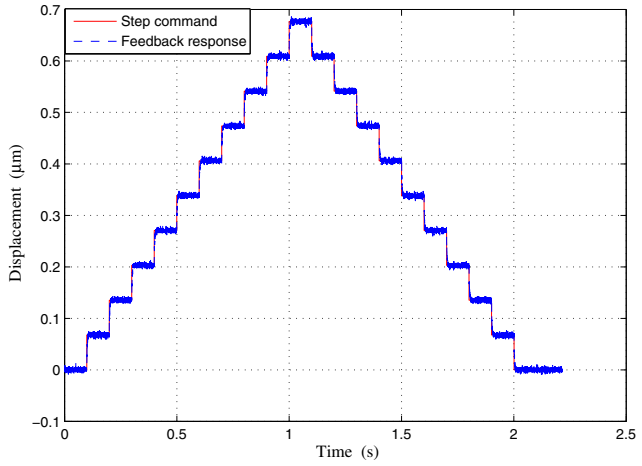

(a) Trajectory tracking(solid-reference trajectory, dash-actual trajectory).

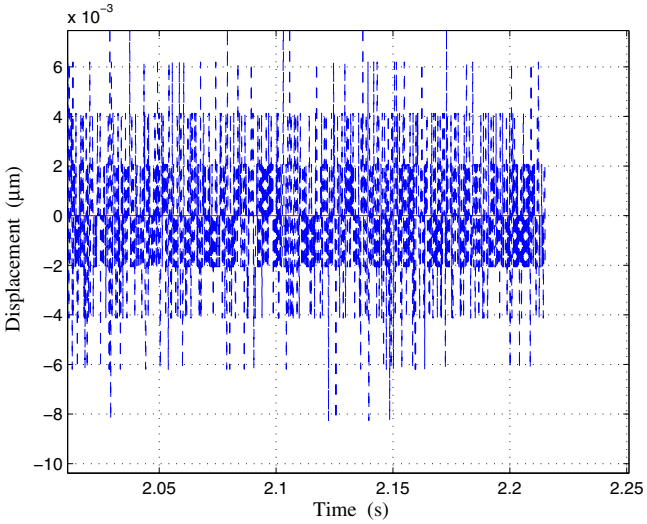

(b) Positioning resolution.

FIG. 7. (Color online) The feedback response for the step command using the PID controller alone. (Top) Trajectory tracking

A. Feedback controller design

In the absence of the analytical dynamic model on the plant, the PID algorithm is a good choice for controller design.[9] In this work, the discrete PID control algorithm is used as follows:

$$u(kT) = k_p e(kT_s) + k_i \sum e(kT_s) + k_d\{e(kT_s) - e[(k-1)T_s]\}, \tag{3}$$

where k_p, k_i, k_d are the proportional gain, integral gain, and derivative gain, respectively, $k(k=1,2,\ldots N)$ is the sample times, and T_s is the sampling time interval. For best performance, the trial and error method is adopted to obtain optimum PID parameters. As discussed in Ref. 35, the creep can be compensated by a PID feedback controller. For this purpose, a step command is applied in the feedback system. Figure 7 shows the feedback response of the micropositioning stage. Comparing with Fig. 1, the creep is completely compensated by the PID controller. Subsequently, we focus on the hysteresis compensation of the piezoelectric actuators in the remainder of this paper.

In the micropositioning stage system, the SGPS can achieve subnanometer resolution and the friction or stiction can be neglected by using the flexure hinge guidance. The system resolution is mainly limited by the 16-bit ADC. The 16-bit ADC of the DSPACE board provides ±10 V measuring range and the minimum voltage that the ADC can take in is given as

$$U_{\min} = \frac{20}{2^{16}}(\mathrm{V}) \approx 0.305\ 18(\mathrm{mV}). \tag{4}$$

Therefore, the positioning resolution of the system is calculated as about $0.305\ 18/0.148 \approx 2.07$ nm. In practical applications, the electronics-induced noise and the length of the connecting cables also influence the positioning resolution. The actual positioning error of the system is shown in Fig. 7(b). If a zero-phase low-pass filter[4] is used to attenuate higher frequency noisy signals, the actual positioning accuracy can be improved, which is not the focus of this paper.

B. Feedforward controller design

The feedforward controller is designed to predict and linearize the rate-dependent hysteresis in piezoelectric actuators based on the developed hysteresis model. According to Remark 1 and Eq. (2), the discrete hysteresis function $H[u] \times (kT_s)$ and the discrete inverse hysteresis function $H^{-1}[y] \times (kT_s)$ are derived as follows:

$$y(kT_s) = H[u](kT_s) = p_1(u_A,f)u(kT_s) + p_2(u_A,f)u[(k-1)T_s] + p_3(u_A,f), \tag{5}$$

$$u(kT_s) = H^{-1}[y](kT_s) = p_1'(y_A,f)y(kT_s) + p_2'(y_A,f)u[(k-1)T_s] + p_3'(y_A,f), \tag{6}$$

where $p_i(u_A,f), i \in [1,3]$ are the coefficients with respect to the amplitude and frequency of the input voltage and $p_i'(y_A,f), i \in [1,3]$ are the coefficients with respect to the amplitude and frequency of the reference trajectory. The details of the mathematical analysis can be seen in the Appendix.

Remark 2. *For a given input* $u(kT_s) \in C[0,T]$ *with* $k=1,2,\ldots N$; $N=T/T_s$, *the rate-dependent hysteresis function* $H[u](kT_s)$ *can be described by a continuous one-to-one mapping* $\Gamma\{u(kT_s), u[(k-1)T_s]; y(kT_s)\}: R^2 \to R$, *such that* $H[u] \times (kT_s) = p_1(u_A,f)u(kT_s) + p_2(u_A,f)u[(k-1)T_s] + p_3(u_A,f)$.

Remark 3. *For a given reference trajectory* $y(kT_s) \in C[0,T]$ *with* $k=1,2,\ldots N$; $N=T/T_s$, *the rate-dependent inverse hysteresis function* $H^{-1}[y](kT_s)$ *can be described by a continuous one-to-one mapping* $\Gamma^{-1}\{y(kT_s), y[(k-1)T_s]; u(kT_s)\}: R^2 \to R$, *such that* $H^{-1}[y](kT_s) = p_1'(y_A,f)y(kT_s) + p_2'(y_A,f)y[(k-1)T_s] + p_3'(y_A,f)$.

In order to validate the inverse hysteresis model, simulation results are compared with the experimental data under the sinusoidal excitations as shown in Fig. 8. The results show that the inverse model can be used to develop feedforward controller for canceling the rate-dependent hysteresis. Then, the coefficients of the inverse hysteresis model are identified for real-time feedforward controller design. Figure 9 illustrates the relation curves of coefficients with varying the input amplitudes under different frequencies. The results

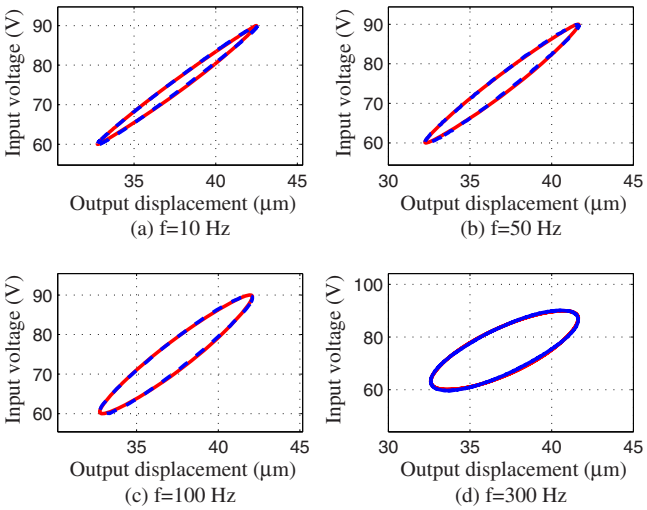

FIG. 8. (Color online) Comparisons of the inverse hysteresis curves between the experimental results and the simulation results predicted by the inverse hysteresis model under the sinusoidal excitations of $u(t)=75+15\sin(2\pi ft)$ (solid–experimental data; dash–inverse model simulation).

show that the rates of the coefficients are different from each other according to different input frequencies, which indicates the rate-dependent hysteresis. The figures also demonstrate that the coefficients are nonlinear to the input amplitudes, which describe the amplitude-dependent hysteresis. When the input amplitudes are lower than 10 μm, the coefficients can be represented by quadratic functions of the input amplitudes under a fixed frequency. Otherwise, the coefficients are linear to the input amplitudes when the input frequency is constant. It should be mentioned that the order of the coefficient $p_3'(y_A,f)$ is not sequential with varying frequencies due to the modeling errors and parameter uncertainties. Therefore, the feedforward compensation strategy would result in tracking biases comparing with the reference trajectory, which is verified in the experimental tests. In fact, a hybrid controller can easily eliminate the uncertainties, which will be discussed in detail in the following sections. In addition, because of the structural vibration of the stage,[19] there may be anomalies when the amplitudes are large under frequencies higher than 150 Hz. However, we focus on compensating for the rate-dependent hysteresis in this work. The structural vibration is not addressed in this paper.

V. EXPERIMENTAL TESTS

As periodic sinusoid waveforms are commonly used as desired trajectories for tracking control applications of piezoelectric actuators,[9,11,14] we use the sinusoid waveforms as the reference trajectories in this work. We conducted sets of comparison experiments. We first apply the feedforward tracking control using the inverse hysteresis model. Then, we discuss the feedback tracking control results only with the PID controller. Finally, we adopt the feedforward controller in conjunction with the PID feedback loop for tracking control of the piezoelectric actuators.

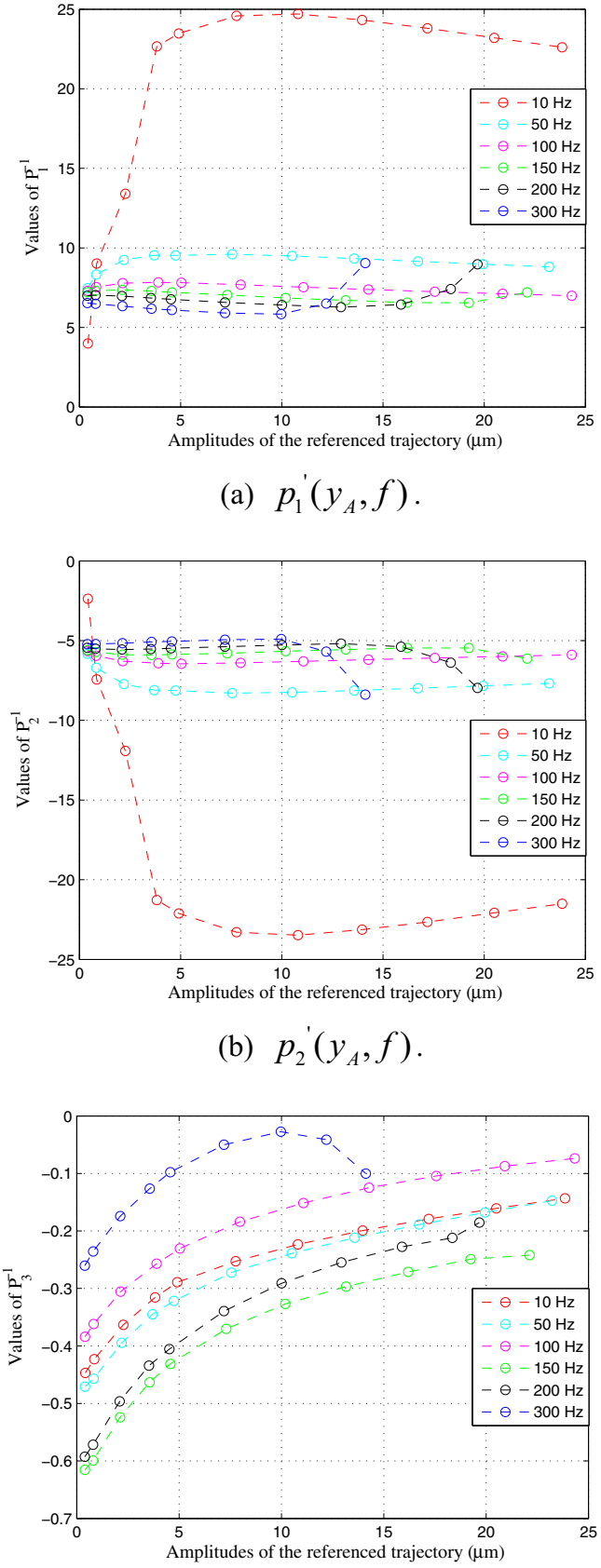

(a) $p_1'(y_A,f)$.

(b) $p_2'(y_A,f)$.

(c) $p_3'(y_A,f)$.

FIG. 9. (Color online) The coefficients of the inverse hysteresis model under different input amplitudes and frequencies.

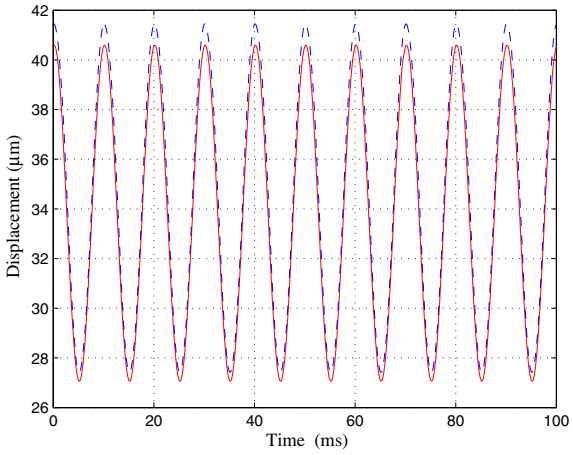

(a) Trajectory tracking(solid-reference trajectory, dash-actual trajectory).

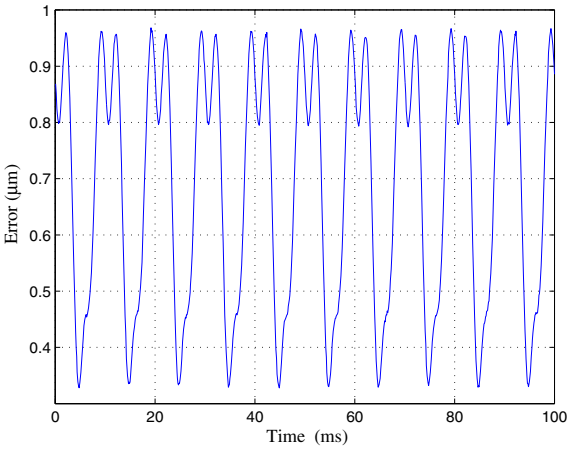

(b) Tracking error.

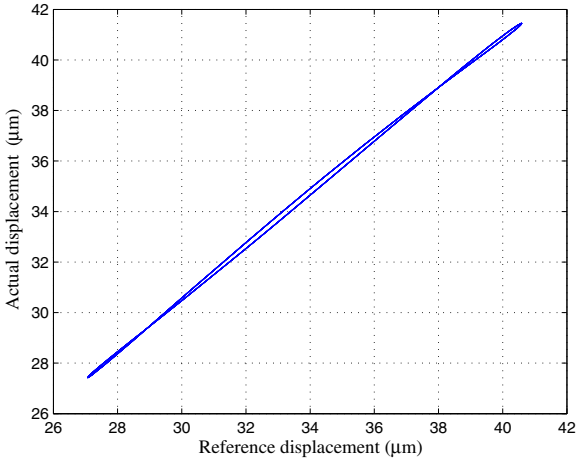

(c) Resulting hysteresis curves.

FIG. 10. (Color online) Feedforward tracking control at the input frequency of 100 Hz.

A. Feedforward tracking control

The feedforward controller was designed based on the inverse hysteresis model to cancel the hysteresis in the piezoelectric actuators. The first experimental test was conducted to track the sinusoidal trajectory in the frequency of 100 Hz when $u_f(kT)$ was zero. Figure 10 shows the feedforward tracking control response. As described in Fig. 10(c), the resulting hysteresis height error (HHE) is reduced by up to 88% comparing with the open loop response as illustrated in Fig. 11. However, the inverse model-based feedforward controller lacks robustness and is sensitive to the modeling errors and parameter uncertainties. Therefore, the actual trajectory has a positive tracking bias illustrated in Fig. 10(a), and the maximum tracking error is about 0.97 μm as shown in Fig. 10(b). Actually, these errors can be eliminated easily by a feedback controller using the actual output trajectory deviations from the reference trajectory, which will be discussed in the following paragraph.

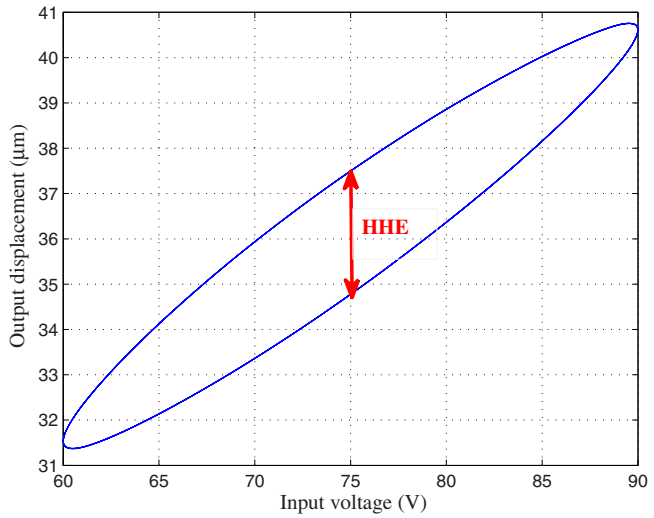

FIG. 11. (Color online) Open loop response at the input frequency of 100 Hz.

B. Feedback tracking control

This set of experiments was conducted by only using the PID feedback loop when $u_f(kT)$ equaled zero. As shown in Fig. 7, the PID controller can obviously remove the creep and hysteresis effects for the step command. Figure 12 shows the comparison of the reference trajectory and the actual output trajectory under the frequency of 1 Hz. The results demonstrate that the PID controller can compensate for the hysteresis at the lower frequency as shown in Fig. 12(c). However, the control performance of the PID controller is bad when the input frequency is high. Figure 13 shows the comparison results at the input frequency of 100 Hz. It is obvious that the tracking performance is severely degraded when we only use the PID controller and the maximum tracking error can be about 8.2% of the travel range. Figure 13(c) also demonstrates that the PID controller cannot compensate for the hysteresis at the high input frequency. In other words, the pure feedback controller cannot work well for high-speed tracking control.

C. Hybrid tracking control

Figure 14 shows the tracking control results when both the feedforward controller and the feedback loop are used. Figure 14(c) demonstrates that the feedback-feedforward

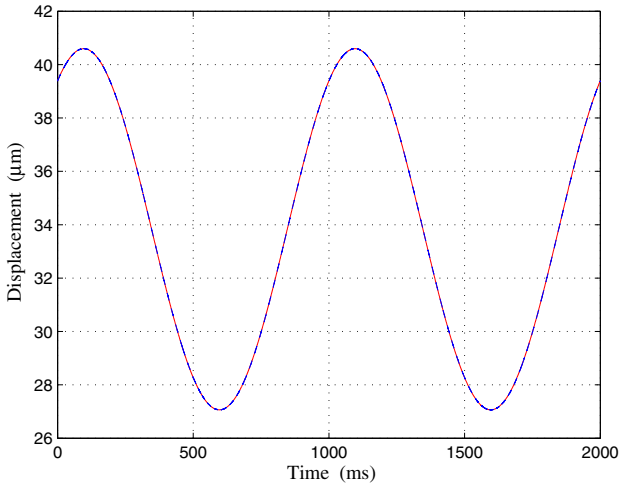

(a) Trajectory tracking(solid-reference trajectory, dash-actual trajectory).

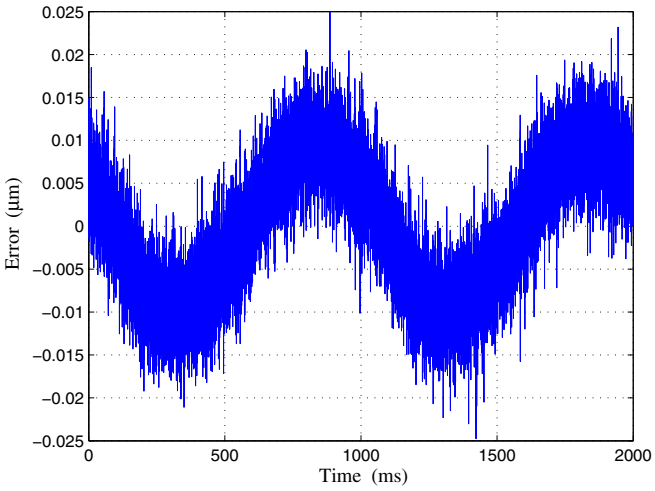

(b) Tracking error.

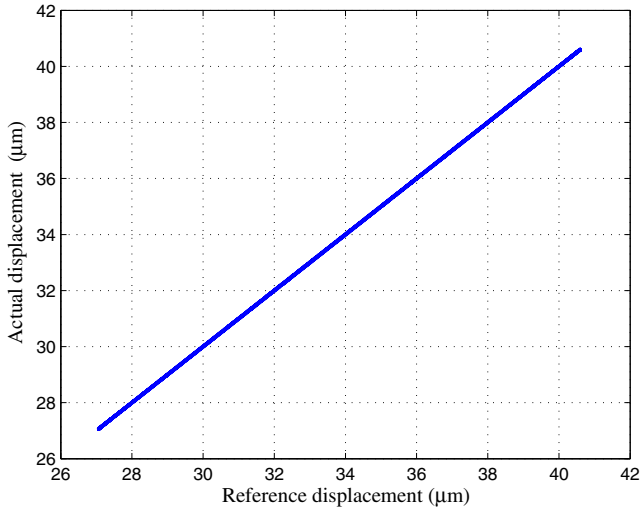

(c) Resulting hysteresis curves.

FIG. 12. (Color online) Feedback tracking control at the input frequency of 1 Hz.

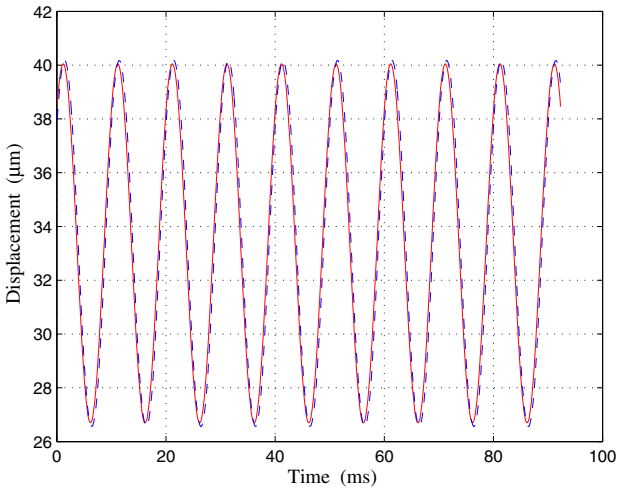

(a) Trajectory tracking(solid-reference trajectory, dash-actual trajectory).

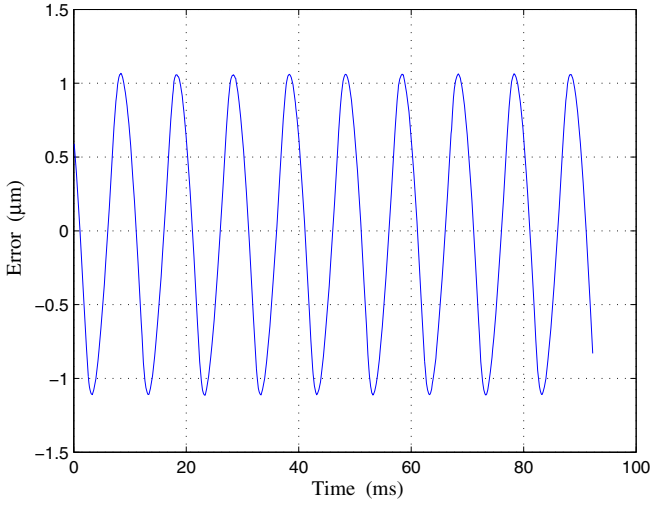

(b) Tracking error.

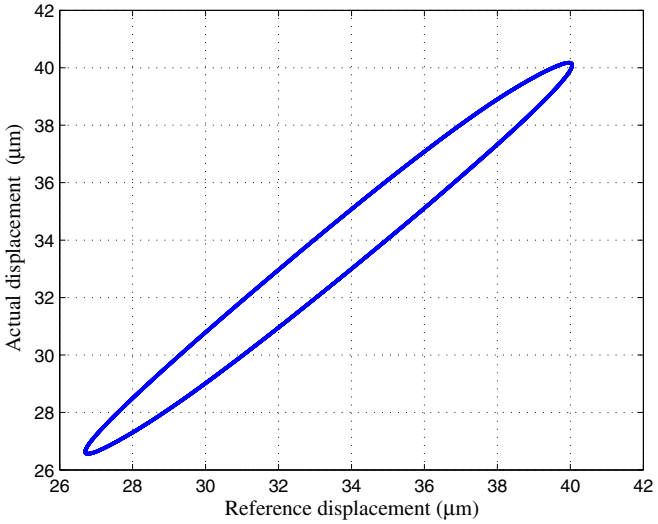

(c) Resulting hysteresis curves.

FIG. 13. (Color online) Feedback tracking control at the input frequency of 100 Hz.

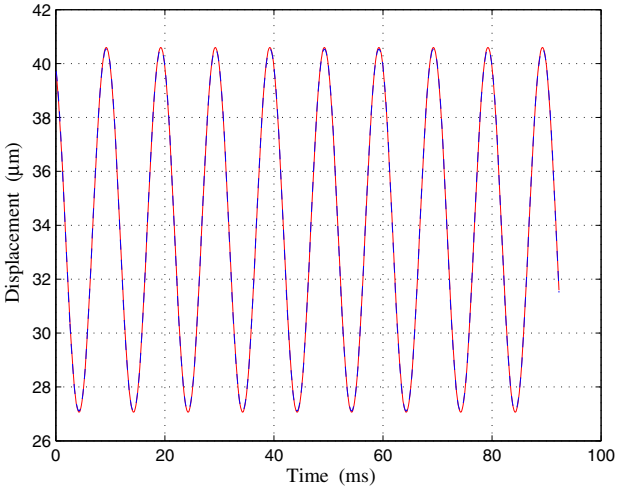

(a) Trajectory tracking(solid-reference trajectory, dash-actual trajectory).

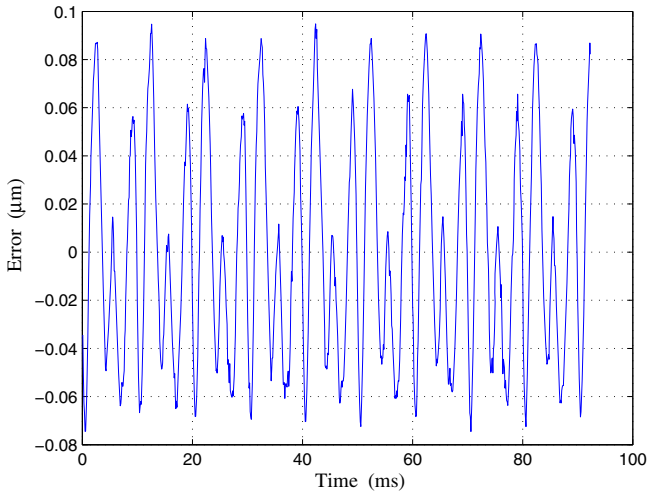

(b) Tracking error.

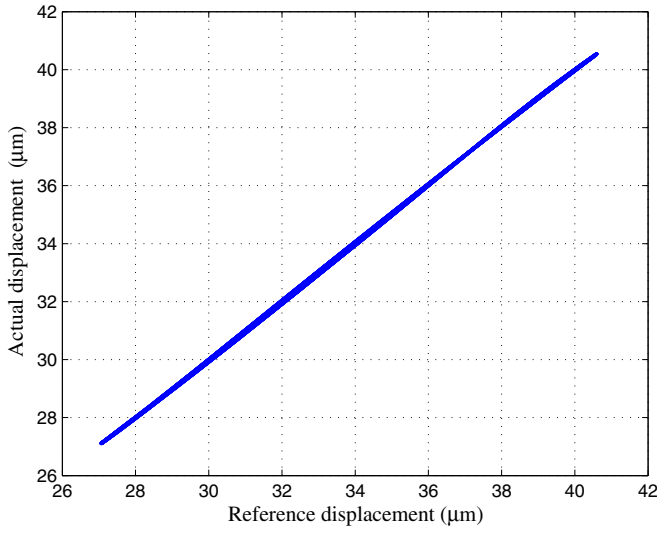

(c) Resulting hysteresis curves.

FIG. 14. (Color online) Hybrid tracking control at the input frequency of 100 Hz.

TABLE I. Tracking performance of different controllers at the input frequency of 100 Hz (values reported by the percentage of the displacement range).

Controller	MTE (%)	RMSTE (%)
Feedforward[a]	7.16	5.33
PID	8.2	5.53
Hybrid	0.7	0.34

[a]Reference 36.

control strategy well compensates for the multivalued hysteresis effect. The maximum tracking error is less than 0.1 μm, which is about 0.7% of the moving range. In Table I, the tracking performance of different controllers is summarized with respect to the maximum tracking error (MTE) and the root-mean-square tracking error (RMSTE). Table II shows the variations of the tracking performance under different frequencies. Apparently, the tracking performance is greatly improved by incorporating hysteresis compensation in the feedforward path. On one hand, compared with the PID control method, the hybrid control strategy reduces the MTE and RMSTE by above 80% when the input frequencies are higher than 10 Hz. On the other hand, we observe that the tracking performance falls down with increasing frequencies. Song *et al.*[20] achieved the average tracking performance of 2.5% of the moving range when the input frequency is only 0.01 Hz in their experiments. It is clear that our proposed hysteresis model greatly improves the tracking accuracy in piezoelectric actuators, especially for high-speed tracking control.

VI. CONCLUSION

In this paper, an ellipse-based model is proposed to characterize the rate-dependent hysteresis in piezoelectric actuators. Based on the developed model, a real-time model-based feedforward controller is developed to cancel the hysteresis. This approach has been shown to reduce the hysteresis error by up to 88%. However, the feedforward controller lacks robustness and is sensitive to the modeling errors and

TABLE II. Tracking performance of PID and hybrid controllers with different frequencies (values reported by the percentage of the displacement range).

Frequency (Hz)	Controller	MTE (%)	RMSTE (%)
1	PID	0.18	0.06
	Hybrid	0.14	0.03
10	PID	0.79	0.5
	Hybrid	0.16	0.04
50	PID	3.76	2.6
	Hybrid	0.41	0.17
300	PID	41.17	28.19
	Hybrid	3.22	1.68

parameter uncertainties. Therefore, a PID feedback loop is also proposed to compensate for the creep, modeling errors, and parameter uncertainties. Experimental results demonstrate that the tracking control performance is greatly improved in high-speed applications using the hybrid control scheme.

ACKNOWLEDGMENTS

This work was partially supported by the Science and Technology Commission of Shanghai Municipality under Grant Nos. 09520701700 and 09JC1408300, and the National Key Basic Research Program under Grant No. 2007CB714005.

APPENDIX: MATHEMATICAL DERIVATION OF EQS. (5) AND (6)

According to Eq. (2), for a given input in the form of $u(t)=u_0+u_A \sin(2\pi ft)$, the output can be obtained as follows:

$$\begin{aligned} y(t) &= y_0 + y_A \sin(2\pi ft + \alpha_2 - \alpha_1) \\ &= y_0 + y_A \sin(2\pi ft)\cos(\alpha_2 - \alpha_1) \\ &\quad + y_A \cos(2\pi ft)\sin(\alpha_2 - \alpha_1) \\ &= y_0 + y_A \cos(\alpha_2 - \alpha_1)[u(t) - u_0]/u_A \\ &\quad + y_A \sin(\alpha_2 - \alpha_1)\dot{u(t)}/(u_A 2\pi f). \end{aligned} \tag{A1}$$

For the numerical controller implementation, the input and output signals are sampled with the constant period. The sampling time interval is denoted as T_s and time is set to $t=kT_s$ with k being an integer. Therefore, the discrete output $y(kT_s)$ is

$$\begin{aligned} y(kT_s) &= y_0 + y_A \cos(\alpha_2 - \alpha_1)[u(kT_s) - u_0]/u_A \\ &\quad + [y_A \sin(\alpha_2 - \alpha_1)/(u_A 2\pi f)]u(\dot{kT_s}). \end{aligned} \tag{A2}$$

Here, the derivative of the input $u(kT_s)$ is approximated as

$$u(\dot{kT_s}) = \{u(kT_s) - u[(k-1)T_s]\}/T_s. \tag{A3}$$

Substituting Eq. (A3) into Eq. (A2), we get

$$y(kT_s) = p_1(u_A,f)u(kT_s) + p_2(u_A,f)u[(k-1)T_s] + p_3(u_A,f). \tag{A4}$$

Without loss of generality, for a given output in the form of $y(kT_s)=y_0+y_A \sin(2\pi fkT_s)$, the discrete input $u(kT_s)$ can be obtained as follows:

$$u(kT_s) = p_1'(y_A,f)y(kT_s) + p_2'(y_A,f)y[(k-1)T_s] + p_3'(y_A,f). \tag{A5}$$

[1] Y. Li and J. Bechhoefer, Rev. Sci. Instrum. **78**, 013702 (2007).
[2] G. M. Clayton, S. Tien, K. K. Leang, Q. Zou, and S. Devasia, J. Dyn. Syst., Meas., Control **131**, 061101 (2009).
[3] B. Mokaberi and A. A. G. Requicha, IEEE Trans. Autom. Sci. Eng. **5**, 197 (2008).
[4] D. A. Bristow, J. Dong, A. G. Alleyne, P. Ferreira, and S. Salapaka, Rev. Sci. Instrum. **79**, 103704 (2008).
[5] H. Xie, M. Rakotondrabe, and S. Regnoer, Rev. Sci. Instrum. **80**, 046102 (2009).
[6] H. Jung and D. G. Gweon, Rev. Sci. Instrum. **71**, 1896 (2000).
[7] H. Jung, J. Y. Shim, and D. Gweon, Rev. Sci. Instrum. **71**, 3436 (2000).
[8] S. O. R. Moheimani, Rev. Sci. Instrum. **79**, 11 (2008).
[9] P. Ge and M. Jouaneh, IEEE Trans. Control Syst. Technol. **4**, 209 (1996).
[10] U. X. Tan, W. T. Latt, F. Widjaja, C. Y. Shee, C. N. Riviere, and W. T. Ang, Sens. Actuators, A **150**, 116 (2009).
[11] M. Al Janaideh, S. Rakheja, and C. Y. Su, Mechatronics **19**, 656 (2009).
[12] C. V. Newcomb and I. Flinn, Electron. Lett. **18**, 442 (1982).
[13] S. Devasia, E. Eleftheriou, and S. O. R. Moheimani, IEEE Trans. Control Syst. Technol. **15**, 802 (2007).
[14] G. S. Choi, Y. A. Lim, and G. H. Choi, Mechatronics **12**, 669 (2002).
[15] C. Y. Su, Y. Stepanenko, J. Svoboda, and T. P. Leung, IEEE Trans. Autom. Control **45**, 2427 (2000).
[16] H. Janocha and K. Kuhnen, Sens. Actuators, A **79**, 83 (2000).
[17] J. W. Macki, P. Nistri, and P. Zecca, SIAM Rev. **35**, 94 (1993).
[18] H. Adriaens, W. L. de Koning, and R. Banning, IEEE/ASME Trans. Mechatron. **5**, 331 (2000).
[19] K. K. Leang and S. Devasia, Proceedings of the Second IFAC Conference on Mechatronic Systems, 2002, pp. 283–289.
[20] G. Song, J. Q. Zhao, X. Q. Zhou, and J. A. de Abreu-Garcia, IEEE/ASME Trans. Mechatron. **10**, 198 (2005).
[21] Q. Q. Wang and C. Y. Su, Automatica **42**, 859 (2006).
[22] D. Croft and S. Devasia, J. Guid. Control Dyn. **21**, 710 (1998).
[23] C. H. Ru and L. N. Sun, Rev. Sci. Instrum. **76**, 095111 (2005).
[24] S. Bashash and N. Jalili, ASME J. Dyn. Syst., Meas., Control **130**, 031008 (2008).
[25] J. M. Cruz-Hernandez and V. Hayward, IEEE Trans. Control Syst. Technol. **9**, 17 (2001).
[26] Y. H. Yu, Z. C. Xiao, N. G. Naganathan, and R. V. Dukkipat, Mech. Mach. Theory **37**, 75 (2002).
[27] M. Al Janaideh, S. Chun-Yi, and S. Rakheja, Smart Mater. Struct. **17**, 035026 (2008).
[28] U. X. Tan, W. T. Latt, C. Y. Shee, C. N. Riviere, and W. T. Ang, IEEE/ASME Trans. Mechatron. **14**, 598 (2009).
[29] D. Croft and S. Devasia, Rev. Sci. Instrum. **70**, 4600 (1999).
[30] S. S. Aphale, S. Devasia, and S. O. R. Moheimani, Nanotechnology **19**, 125503 (2008).
[31] F. Dufrenois, Proceedings of the Sixth European Conference on Symbolic and Quantitative Approaches to Reasoning with Uncertainty, 2001, pp. 432–443.
[32] M. Schneider, J. Liszkowski, M. Rahm, W. Wegscheider, D. Weiss, H. Hoffmann, and J. Zweck, J. Phys. D: Appl. Phys. **36**, 2239 (2003).
[33] E. Della Torre, E. Pinzaglia, and E. Cardelli, Physica B **372**, 115 (2006).
[34] G. Y. Gu and L. M. Zhu, Proceedings of the IEEE/ASME International Conference on Advanced Intelligent Mechatronics, 2010.
[35] H. Jung, J. Y. Shim, and D. Gweon, Nanotechnology **12**, 14 (2001).
[36] When the feedforward controller is used alone, there is a positive tracking error bias as shown in Fig. 10(b). That is caused by the modeling errors and parameter uncertainties. However, the hysteresis height is reduced to only about 2 as illustrated in Fig. 10(c).